Journal of Chromatographic Science 2013;51:8–16
doi:10.1093/chromsci/bms097 Advance Access publication June 11, 2012

Article

Enantioseparation and Chiral Recognition of α-Cyclohexylmandelic Acid and Methyl α-Cyclohexylmandelate on Hydroxypropyl-β-Cyclodextrin as Chiral Selector: HPLC and Molecular Modeling

Jie-hua Shi[1,2*], Yan-hui Su[1] and Wei Jiang[1]

[1]College of Pharmaceutical Sciences, Zhejiang University of Technology, Hangzhou 310032, China, and [2]State Key Laboratory Breeding Base of Green Chemistry Synthesis Technology, Zhejiang University of Technology, Hangzhou 310032, China

*Author to whom correspondence should be addressed. Email: shijh@zjut.edu.cn

Received 17 December 2011; revised 24 April 2012

Enantioseparations of (*R*/*S*)-α-cyclohexylmandelic acid [(*R*/*S*)-CHMA] and methyl (*R*/*S*)-α-cyclohexylmandelate [(*R*/*S*)-MCHMA] were performed on an achiral column (ODS) with 2-hydroxypropyl-β-cyclodextrin (HP-β-CD) as a chiral mobile phase additive. The influences of chromatographic conditions on the retention behavior of (*R*/*S*)-CHMA and (*R*/*S*)-MCHMA were studied in detail. Meanwhile, the thermodynamics parameters of enantioseparations for (*R*/*S*)-CHMA and (*R*/*S*)-MCHMA were determined to discuss driven power in the enantioseparation process. The inclusion complexation of HP-β-CD with each enantiomer for (*R*/*S*)-CHMA and (*R*/*S*)-MCHMA was simulated by molecular docking to understand the chiral recognition mechanism of (*R*/*S*)-CHMA and (*R*/*S*)-MCHMA on HP-β-CD. The results showed that the chiral recognition ability of enantiometers of (*R*/*S*)-CHMA and (*R*/*S*)-MCHMA on HP-β-CD is better than α-CD, β-CD, γ-CD and DM-β-CD. Under the selected chromatographic conditions, baseline separations of enantiomers of (*R*/*S*)-CHMA and (*R*/*S*)-MCHMA were achieved. It is proved that the stoichiometry for (*R*/*S*)-CHMA–HP-β-CD and (*R*/*S*)-MCHMA–HP-β-CD complexes is 1:1. However, the results of thermodynamics parameters analysis and molecular modeling show that the enantioseparations of CHMA and MCHMA on HP-β-CD are enthalpy-driven processes and the primary driving forces responsible for chiral recognition are hydrophobic forces, dipole-dipole interaction, charge-transfer and hydrophobic interaction.

Introduction

α-Cyclohexylmandelic acid (CHMA) and methyl α-cyclohexylmandelate (MCHMA) are important pharmaceutical precursors that can be used as raw materials for producing multiple drugs, such as cyclandelate and oxybutynin with biological activity and good curative effect (1, 2). It is well known that the enantiomers of chiral drugs usually show different bioactivity in the human body. For example, (*S*)-oxybutynin has better pharmacological actions and lower side effects than its racemic mixture (2). Therefore, the enantioseparation of CHMA and MCHMA is necessary for producing chiral drugs, assessing the pharmacokinetic attributes of each enantiomer and controlling the enantiomeric purity of pharmaceutical preparations.

At present, several methods for the enantioseparations of (*R*/*S*)-CHMA and (*R*/*S*)-MCHMA have been reported. Tang *et al.* (3, 4) reported that enantiomers of CHMA were separated in a two-phase extraction system. Guo *et al.* (5) utilized enantioselective liquid–liquid extraction to study the effect of the concentration of 2-hydroxypropyl-β-cyclodextrin (HP-β-CD), the concentration of CHMA, the mass fractions of C_2H_5OH and $(NH_4)_2SO_4$, temperature and pH value on the chiral recognizition of CHMA enantiomers. Huang *et al.* (6, 7) reported the enantioseparation of racemic CHMA containing copper(II) N-dodecyl-(L)-hydroxyproline (CuN_2) as a chiral carrier using hollow fiber-supported liquid membrane. Feitsma *et al.* (8) investigated the enantioseparation and elution order of CHMA on two β-CD bonded stationary phases using high-performance liquid chromatography (HPLC) and found that the elution order of the optical isomers is different on the two columns. We recently reported the enantioseparation of methyl mandelate (MMA) and MCHMA on permethylated β-cyclodextrin (PM-β-CD) chiral stationary phase (9). The chromatographic separation of enantiomers of chiral compounds is a very efficient method for evaluting the pharmacokinetic attributes of each enantiomer and determining the enantiomeric purity in the process of phamaceutical preparation.

Cyclodextrins and their derivatives have been widely used as chiral selectors in the field of enantioseparation of chiral compounds (10–16). To understand the chiral recognition mechanism underlying the chiral separation using cyclodextrins and their derivatives as chiral selectors, great advances have been made using experimental (17, 18) and theoretical methods (19–24) during the past decade. However, to the best of our knowledge, the chiral recognition mechanism of CHMA and MCHMA on HP-β-CD has not yet been reported.

The goal of this work was to establish a method for the enantioseparation of CHMA or MCHMA using cyclodextrins (CDs) as chiral mobile phase additive and to understand chiral recognition mechanism at the molecular level via the molecular modeling. To achieve our goal, the effect of chromatographic conditions (such as type and concentration of CD additive, pH, content of methanol and column temperature) on the enantionseparation of CHMA and MCHMA was first researched. Second, the thermodynamic parameters in the process of enantioseparations of CHMA and MCHMA using HP-β-CD as chiral additive were determined to discuss the driven power in the process of enantioseparations. Third, the interaction of HP-β-CD with enantiomers of CHMA and MCHMA was simulated by the molecular docking method and natural bond orbital (NBO) analysis was performed to discover why and how the chiral recognition takes place.

Materials and Methods

Chemicals

α-Cyclodextrin (α-CD) and γ-cyclodextrin (γ-CD) were purchased from Wuhan Xianghe Corporation (Wuhan, China). β-Cyclodextrin (β-CD) was purchased from Tailong Science & Technology Corporation (Wuhan, China). 2,6-Dimethyl-β-cyclodextrin (DM-β-CD) was purchased from Kunshan Ruisikechemical Raw Material Corporation (Jiangsu, China). HP-β-CD was purchased from Shandong Xinda Fine Chemical Corporation (Shandong, China). (*R*/*S*)-CHMA, (*R*/*S*)-MCHMA, (*R*)-CHMA and (*S*)-MCHMA were provided by College of Pharmaceutical Sciences, Zhejiang University of Technology (Zhejiang, China).

Apparatus

An Agilent 1100 series HPLC with variable wavelength detection (VWD) and a Chemstation workstation was purchased from Agilent Corporation (Santa Clara, CA). A Tigerkin ODS3 column was purchased from Dalian Sipore Corporation (Dalian, China). The solvent filter was purchased from Changcheng Glass Instrument Factory (Anhui, China).

HPLC measurements

The solutes used in this experiment were dissolved by methanol and these solutions were filtered through a 0.22-μm filter before use.

Chromatographic conditions

A mixture of methanol and water containing CDs as chiral additives was used as mobile phase; the flow rate was set at 0.8 mL/min; the sampling volume was 20 μL; the ultraviolet (UV) detection wavelength was 221 nm. Sodium nitrate was used to determine the t_0 value.

Molecular modeling

The starting structures of (*R*/*S*)-CHMA and (*R*/*S*)-MCHMA enantiomers were constructed with the help of Chem 3D Ultra (Version 8.0, CambridgeSoft; Cambridge, MA). These structures were first optimized by the semiempirical PM3 method implemented in the Gaussian 03 and then further optimized by the density functional theory (DFT) implemented in the Gaussian 03 at B3LYP/6-31 + g(d) level until all eigenvalues of the Hessian matrix were positive (25).

Using Chem 3D Ultra, the initial geometry of HP-β-CD was constructed from the crystallographic parameters of β-CD taken from the Cambridge Structureal Database (CSD). The H-atoms in the 2-OH of each glucose unit for β-CD were replaced with 2-hydroxypropyl groups. Similarly, the structure was first optimized by the PM3 method and then further optimized by DFT at the B3LYP/6-31g level until all eigenvalues of the Hessian matrix were positive. The DFT-optimized structures of (*R*/*S*)-CHMA, (*R*/*S*)-MCHMA and HP-β-CD were used for the molecular docking calculations.

The interactions of HP-β-CD with (*R*/*S*)-CHMA and (*R*/*S*)-MCHMA enantiomers were simulated by molecular docking using AutoDock 4.0 (26). The Lamarckian genetic algorithm (LGA) was selected for each enantiomers for the CHMA and MCHMA conformational search, and all parameters were the same for each docking. The partial atomic charges of HP-β-CD and each enantiomer were calculated using the Gasterier-Marsili (27) and Kollman methods (28), respectively. After merging non-polar hydrogen, the rotatable bonds were assigned. The grid maps were then calculated using AutoGrid. A grid map of dimensions $60 \times 60 \times 60$ Å with a grid-point spacing of 0.375 Å was created for each enantiomer, which ensured an appropriate size of the each enantiomer-accessible space (29). The number of genetic algorithm runs for each inclusion complex and the number of evaluations for each run were set to 200 and 2.5 million, respectively. Other docking parameters such as crossover, mutation and elitism were set as default (0.08, 0.02 and 1, respectively). Based on RMS cluster tolerance between structures, the (*R*/*S*)-CHMA–HP-β-CD and (*R*/*S*)-MCHMA–HP-β-CD complexs were sorted into clusters. Finally, we obtained the dominating configuration of (*R*/*S*)-CHMA–HP-β-CD and (*R*/*S*)-MCHMA–HP-β-CD complexes with minimum binding free energy (ΔG).

NBO analysis

NBO analysis for the dominating configuration of inclusion complexes with minimum binding free energy (ΔG) obtained by molecular docking was performed at the B3LYP/6-31g level to obtain information about the intramolecular and intermolecular interactions such as hydrogen bonding, intermolecular charge transfer and dipole-dipole interaction of HP-β-CD with (*R*/*S*)-CHMA and (*R*/*S*)-MCHMA. In the NBO analysis, the electronic delocalization interaction can be quantitatively described using the stabilization energy [$E^{(2)}$], which is estimated by second order perturbation theory. The $E^{(2)}$ can be calculated according to Eq. (1) (30, 31):

$$E^{(2)} = -n_\sigma \frac{\langle \sigma|F|\sigma\rangle}{\varepsilon_{\sigma*} - \varepsilon_\sigma} = -n_\sigma \frac{F_{i,j}^2}{\Delta E} = -n_\sigma \frac{F_{i,j}^2}{E_j - E_i} \quad (1)$$

where $< \sigma|F|\sigma >$denotes the Fock matrix elements between i and j orbitals; $F_{i,j}$ is the off-diagonal NBO Fock matrix element; $\varepsilon_{\sigma*}$ and$\varepsilon_\sigma$are the energies of σ and σ* NBO orbitals, n_σ denotes the population of the donor σ orbital; E_i and E_j denote diagonal elements (orbital energies).

Results and Discussion

Influence of the species of cyclodextrin

The effect of the species of cyclodextrins on the enantioseparations of (*R*/*S*)-CHMA and (*R*/*S*)-MCHMA was evaluated. The experimental results showed that the enantiomers of (*R*/*S*)-CHMA and (*R*/*S*)-MCHMA were efficiently resolved using HP-β-CD as chiral mobile phase additive, but not using other CDs, suggesting that the chiral recognition abilities of CDs for (*R*/*S*)-CHMA and (*R*/*S*)-MCHMA are closely related to the structure of CDs.

However, (*S*)-CHMA was eluted earlier than (*R*)-CHMA, while the (*R*)-MCHMA is eluted earlier than (*S*)-MCHMA, suggesting that the intermolecular interactions of (*S*)-CHMA and (*R*)-MCHMA with HP-β-CD were stronger than that of (*R*)-CHMA and (*S*)-MCHMA, respectively. In other words, the

Table I

Effect of the Concentration of HP-β-CD on the Retention Factors (k'), Separation Factors (α) and Resolutions (R_s) for Enantiomers of CHMA and MCHMA*

$C_{HP\text{-}\beta\text{-}CD}$ (mol/L)	CHMA				MCHMA			
	k'_S	k'_R	α	R_S	k'_R	k'_S	α	R_S
0.005	65.95	72.19	1.09	1.54	161.34	168.68	1.05	0.83
0.010	42.25	47.38	1.12	2.01	108.90	116.93	1.07	1.23
0.015	33.75	38.20	1.13	2.24	85.48	92.22	1.08	1.64
0.020	24.4	27.69	1.13	1.85	63.16	68.91	1.09	0.91

*Note: Column, Tigerkin ODS3; mobile phase, CH_3OH-H_2O (containing 5 ~ 20 mmol/L HP-β-CDs, 20 mmol/L KH_2PO_4 and n mmol/L H_3PO_4, pH 2.5), 40:60 (v/v); flow rate, 0.8 mL/min; column temperature, room temperature; k'_R and k'_S mean the retention factors of (*R*)-isomer and (*S*)-isomer, respectively.

inclusion complexes formed by HP-β-CD with (*S*)-CHMA or (*R*)-MCHMA were more stable than with (*R*)-CHMA or the (*S*)-MCHMA. It is implied that there is an obvious different chiral recognition mechanism of HP-β-CD with enantiomers of CHMA and MCHMA.

Influence of concentration of HP-β-CD

The experimental results concerning the effect of the concentration of HP-β-CD on the retention factors (k'), separation factors (α) and resolution factors (R_S) for the (R/S)-CHMA and (R/S)-MCHMA under the selected conditions are summarized in Table I. Table I shows that when the concentration of HP-β-CD is 15 mmol/L, the enantioseparation degrees of CHMA and MCHMA are better. This may be because the formation of the inclusion complexes of CHMA and MCHMA with HP-β-CD was incomplete, leading to either partial or no resolution of enantiomers while the concentration of HP-β-CD was lower. The increase of the concentration of HP-β-CD can favor the formation of the inclusion complexes. Then, with the further increase of the concentration of HP-β-CD, the self-associated interactions between molecules of HP-β-CD will increase, leading to a reduction of enantioseparation degrees.

In most cases, the inclusion complex formed by the interaction of solute molecule with CDs is 1:1 stoichiometry. In some cases, two or more CD molecule can also associate with a single solute molecule. The relationship between the capacity factor (k') of the solute molecule in the chromatographic system and the concentration of CDs in the case of 1:1 stoichiometry can be expressed as Eq. (2) (32, 33):

$$\frac{1}{k'} = \frac{1}{\phi K C_A} + \frac{K_I C_{CDs}}{\phi K C_A} \quad (2)$$

where K and K_I are the corresponding equilibrium constant for the interaction of the solute molecule with the stationary phase absorption site and the corresponding equilibrium constant for the interaction of solute molecule with CDs, respectively; ϕ denotes the phase ratio; C_A and C_{CDs} mean the stationary phase absorption site surface density or concentration and the concentration of CDs, respectively. The dependence of the reciprocal retention factors ($1/k'$) of (R/S)-CHMA and (R/S)-MCHMA upon concentration of HP-β-CD ($C_{HP\text{-}\beta\text{-}CD}$) is depicted in Figure 1. Figure 1 shows that there is a good linear correlation between $1/k'$ and $C_{HP\text{-}\beta\text{-}CD}$ over the entire concentration range studied, which is shown in Eqs. (3) to (6). It is indicated that the complexes of (R/S)-CHMA and (R/S)-MCHMA with HP-β-CD

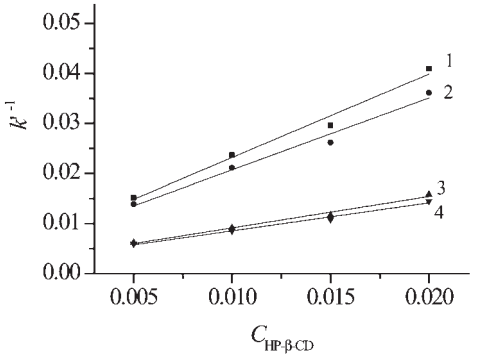

Figure 1. Reciprocal retention factors of the enantiomers of CHMA and MCHMA upon concentration of HP-β-CD: 1, (*S*)-CHMA; 2, (*R*)-CHMA; 3, (*R*)-MCHMA; 4, (*S*)-MCHMA.

Table II

Effect of Methanol Content of on the Retention Factors (k'), Separation Factors (α) and Resolutions (R_S) for Enantiomers of CHMA and MCHMA*

CMeOH (% v/v)	CHMA				MCHMA			
	k'_S	k'_R	α	R_S	k'_R	k'_S	α	R_S
40	33.73	38.17	1.13	2.19	85.49	92.16	1.08	1.69
45	28.08	31.55	1.12	1.60	77.90	82.74	1.06	1.31
55	15.26	16.59	1.09	1.10	35.18	36.24	1.03	—
60	10.11	10.72	1.06	0.76	21.93	21.93	1.00	0

*Note: Column, Tigerkin ODS3; mobile phase, CH_3OH-H_2O (containing 5 ~ 20 mmol/L HP-β-CDs, 20 mmol/L KH_2PO_4 and n mmol/L H_3PO_4, pH 2.5), 40:60 (v/v); flow rate, 0.8 mL/min; column temperature, room temperature; k'_R and k'_S mean the retention factors of (*R*)-isomer and (*S*)-isomer, respectively.

with 1:1 stoichiometry are formed by inclusion interaction. Additionally, the apparent stability constants of (*R*)-CHMA and (*S*)-CHMA upon complexation with HP-β-CD are $(2.3 \pm 0.6) \times 102\ M^{-1}$ and $(2.6 \pm 0.8) \times 102\ M^{-1}$, respectively, as the apparent stability constants of (*R*)-MCHMA–HP-β-CD and (*S*)-MCHMA–HP-β-CD are $(2.2 \pm 0.5) \times 102$ and $(1.9 \pm 0.4) \times 102\ M^{-1}$, respectively, at the selected chromatographic conditions. It is generally suggested that the chiral discrimination ability of chiral compounds on HP-β-CD is primarily based on the difference in the stability constant of each enantiomer upon complexation with CDs:

$$\frac{1}{k'_{S,CHMA}} = (0.00651 \pm 0.0019) + (1.66 \pm 0.14) C_{HP-\beta-CD} \quad (r = 0.9889) \quad (3)$$

$$\frac{1}{k'_{R,CHMA}} = (0.00635 \pm 0.0018) + (1.44 \pm 0.13) C_{HP-\beta-CD} \quad (r = 0.9876) \quad (4)$$

$$\frac{1}{k'_{R,MCHMA}} = (0.00287 \pm 0.00064) + (0.628 \pm 0.046) C_{HP-\beta-CD} \quad (r = 0.9917) \quad (5)$$

$$\frac{1}{k'_{S,MCHMA}} = (0.00295 \pm 0.00056) + (0.561 \pm 0.041) C_{HP-\beta-CD} \quad (r = 0.9921) \quad (6)$$

Influence of content of methanol in mobile phase

As shown in Table II, the k', α and R_S for (R/S)-CHMA and (R/S)-MCHMA resolved on Tigerkin ODS3 using HP-β-CD as

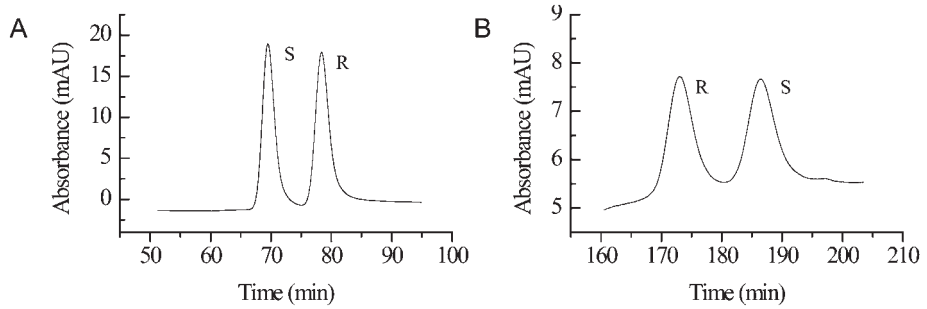

Figure 2. Chromatograms of enantioseparations of CHMA (A); MCHMA (B). Separation was performed on an ODS3 column with CH_3OH:H_2O (containing 15 mmol/L HP-β-CD and 20 mmol/L KH_2PO_4–H_3PO_4, pH 2.5), 40:60 (v/v) used as mobile phase; flow rate 0.8 mL/min; room temperature.

chiral mobile phase additive all decreased with the increase of methanol content in the mobile phase, indicating that methanol content in the mobile phase obviously affects the stability constant of (*R*/*S*)-CHMA and (*R*/*S*)-MCHMA upon complexation with HP-β-CD. This may be because hydrophobic interactions between the solute and the stationary phase are decreased with the increase of methanol content. Meanwhile, at higher methanol contents, methanol competes with solute for preferred locations in the hydrophobic cavity and hydroxypropyl moieties of HP-β-CD, leading to weakening of the affinity of the solute with HP-β-CD (34). As a result, the chiral recognition abilities of (*R*/*S*)-CHMA and (*R*/*S*)-MCHMA on HP-β-CD decrease with the increase of methanol content.

Table III
Effect of pH Value of the Mobile Phase on the Retention Factors (*k*′), Separation Factors (α) and Resolutions (R_S) for Enantiomers of CHMA and MCHMA*

pH	CHMA				MCHMA			
	k'_S	k'_R	α	R_S	k'_R	k'_S	α	R_S
2.5	33.74	38.19	1.13	2.03	83.08	87.92	1.06	1.49
2.8	32.37	36.55	1.13	1.75	84.48	91.24	1.08	1.56
3.1	25.09	28.04	1.12	1.49	86.25	93.29	1.08	1.64
3.5	23.47	26.01	1.11	1.45	91.54	99.34	1.09	1.71

*Note: Column, Tigerkin ODS3; mobile phase, CH_3OH–H_2O (containing 5 ~ 20 mmol/L HP-β-CDs, 20 mmol/L KH_2PO_4 and *n* mmol/L H_3PO_4, pH 2.5), 40:60 (v/v); flow rate, 0.8 mL/min; column temperature, room temperature; k'_R and k'_S mean the retention factors of (*R*)-isomer and (*S*)-isomer, respectively.

Influence of pH value

As acidic and dipolar solute, the HPLC retention of (*R*/*S*)-CHMA and (*R*/*S*)-MCHMA should be strongly related to the pH of the mobile phase. To better understand the effect of pH value on the retention behaviors and enantioselectivity of (*R*/*S*)-CHMA and (*R*/*S*)-MCHMA enantiomers, the *k*′ and α for (*R*/*S*)-CHMA and (*R*/*S*)-MCHMA were determined in the various pH mobile phases containing HP-β-CD, and the results are shown in Table III.

Table III shows that the retention times and resolutions of (*R*/*S*)-CHMA enantiomers decrease gradually with the increase of pH value in the mobile phase, as the retention times and resolutions of (*R*/*S*)-MCHMA increase gradually with the increase of pH value. The possible reasons for the acidic compound (*R*/*S*)-CHMA may be that one dissociation equilibrium exists in aqueous solution, leading to changing the apparent distribution coefficient of (*R*/*S*)-CHMA between mobile phase and stationary phase with the change of pH value in mobile phase solution. Additionally, the protonation degree of the neutral (*R*/*S*)-MCHMA enantiomers containing ester and hydroxyl moieties may increase with the decrease of pH value. In our experiment, the buffer solution was made of KH_2PO_4 (20 mmol/L) and less H_3PO_4, so the ionic strength of the buffer solution increased from approximately 0.020 to 0.023 as the pH value decreased from 3.5 to 2.5. Therefore, increasing the ionic strength should increase the ion-dipole interaction of the neutral dipolar compound with ion in the mobile phase, with the result that the apparent oil-water partition coefficient of the neutral dipolar compound decreases. A similar phenomenon is also observed at pH = 2 ~ 5 for neutral

Table IV
Relationship Between ln*k* and *T* and Thermodynamic Parameters for the Enantioseparation of CHMA and MCHMA

Compounds		$\ln k' = A/T + B$ (*r*)*			ΔH (cal/mol)	$\Delta S + R\ln\phi$ (cal/mol)	$\Delta(\Delta H)^{\dagger}$ (cal/mol)	$\Delta(\Delta S)^{\ddagger}$ (cal/mol)	$\Delta(\Delta G)^{\S}$ (cal/mol)
		A	B	*r*					
(*R*/*S*)-CHMA	k'_S	614.6	1.512	0.9999	−1,221	3.004	−165.0	−0.311	−73.25
	k'_R	698.1	1.356	0.9995	−1,386	2.694			
(*R*/*S*)-MCHMA	k'_R	484.1	2.833	0.9991	−961.9	5.628	−43.0	0.008	−43.55
	k'_S	505.1	2.836	0.9990	−1,003.6	5.636			

*The equation shows the relationship between ln*k* and *T*, where A equals $\Delta H/R$, B equals $\Delta S + R\ln\phi$, *r* is correlation coefficient. R is gas constant (1.987 cal/mol). The temperature range studied is from 25 to 33°C.
†$\Delta(\Delta H)$ is determined by the calculation of the difference of the enthalpic changes between the second-eluted enantiomer and the first-eluted enantiomer.
‡$\Delta(\Delta S)$ is determined by the calculation of the difference of the entropic changes between the second-eluted enantiomer and the first-eluted enantiomer.
§$\Delta(\Delta G)$ is calculated by $\Delta G = \Delta H - T\Delta S$ at 298 K.

Table V
Energies of the Complexes Obtained from Molecular Docking with AutoDock*

Complexes	ΔG	ΔE_1	ΔE_2	ΔE_3
(*R*)-CHMA–HP-β-CD	−7.62	−7.87	−5.63	−2.24
(*S*)-CHMA–HP-β-CD	−8.04	−8.27	−5.90	−2.35
(*R*)-MCHMA–HP-β-CD	−6.24	−6.98	−6.84	−0.14
(*S*)-MCHMA–HP-β-CD	−5.89	−6.56	−6.51	−0.12

*Note: Units are in kcal/mol. ΔG is binding free energy change in the inclusion process, which is calculated in water solvent using a scoring function (38). ΔE_1 is intermolecular interaction energy, which means the energy of the interaction between HP-β-CD and each enantionmer of CHMA and MCHMA and is a sum of Var der Waals energy, hydrogen bonding energy, desolvation free energy and electrostatic energy. ΔE_2 means the sum of Var der Waals energy, hydrogen bonding energy and desolvation energy. ΔE_3 is electrostatic energy.

andrographolide and dehydroandrographolide containing ester and hydroxyl moieties (35). Hence, retention times of the neutral (*R*/*S*)-MCHMA enantiomers are expected to decline as the pH value decreases.

Influence of column temperature

The experimental results showed that, with the increase of column temperature, the eluting power for (*R*/*S*)-CHMA and (*R*/*S*)-MCHMA increases and the enantioseparation efficiency concomitantly decreases, which can be easily explained by the faster migration of the solute molecules through the chromatographic column and their lower affinity to the stationary phase.

Combining retention time and resolution, chromatographic conditions for better enantioseparation of CHMA and MCHMA were optimized. The optimized chromatographic conditions and chromatogram are shown in Figure 2.

Thermodynamic parameters for enantioseparation

The relationship between the retention parameters (k' or α) and the column temperature (T) in the process of chromatographic enantioseparation can be described by Gibbs–Holmholtz and Van't Hoff equations (9) as follows:

$$\ln k' = \frac{-\Delta H}{\mathrm{R}T} + \frac{\Delta S}{\mathrm{R}} + \ln \phi \quad (7)$$

$$\ln \alpha = \frac{-\Delta(\Delta G)}{\mathrm{R}T} = \frac{-\Delta(\Delta H)}{\mathrm{R}T} + \frac{\Delta(\Delta S)}{\mathrm{R}} \quad (8)$$

where k' and α should be defined as the retention factors and the separation factors, respectively; R and T are gas constant and absolute temperature (K), respectively; ϕ is phase ratio; ΔH and ΔS denote the standard enthalpy and entropy of transfer of enantiomers from the mobile phase to the stationary phase, respectively; $\Delta(\Delta H)$ and $\Delta(\Delta S)$ denote the differences $\Delta H_2 - \Delta H_1$ and $\Delta S_2 - \Delta S_1$, respectively, where subscripts 2 and 1 represent the more and the less retained enantiomers; $\Delta(\Delta G)$ denotes a difference in Gibbs free energy of transfer from the mobile phase to the stationary phase between enantiomers. Therefore, apparent thermodynamic parameters in chromatographic separation process were also calculated from the plots of $\ln k'$ or $\ln\alpha$ versus $1/T$. In most cases, the $\Delta(\Delta H)$ value in enantioseparation process tends to be negative, favoring chiral recognition as temperature decreases, and the corresponding $\Delta(\Delta S)$ value is generally also negative, counteracting chiral

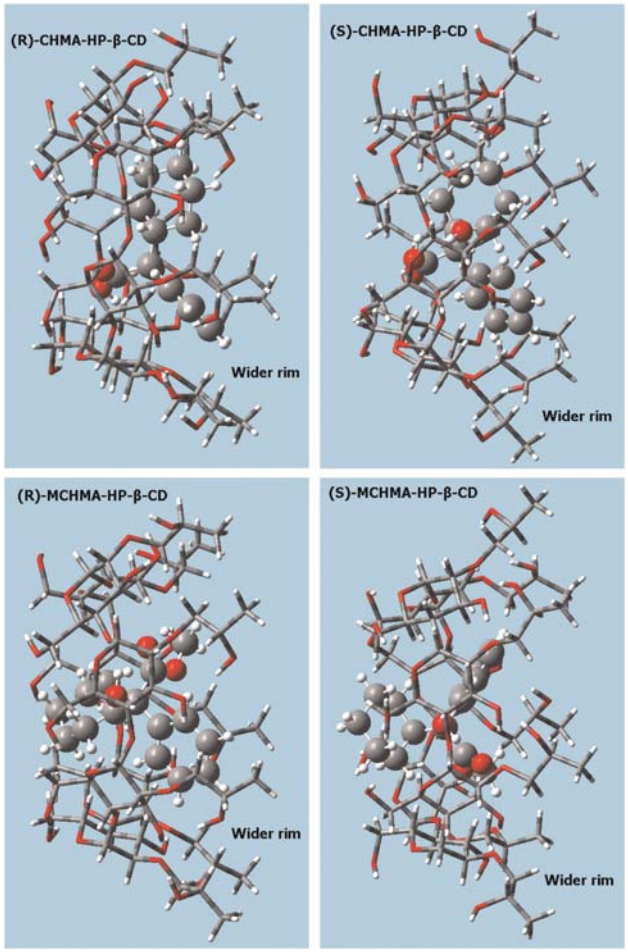

Figure 3. Structures obtained by molecular docking for (*R*/*S*)-CHMA–HP-β-CD and (*R*/*S*)-MCHMA–HP-β-CD complexes.

recognition. This suggests that the enantioseparation is an enthalpy-driven process. Sometimes, the $\Delta(\Delta H)$ and $\Delta(\Delta S)$ for some chiral compounds are both positive, suggesting that the enantioseparation is entropy-driven. If the $\Delta(\Delta H)$ and $\Delta(\Delta S)$ are negative and positive, respectively, the enthalpic and entropic factors are both favorable to chiral recognition (36, 37).

The experimental results showed that the linear relationship between $\ln k'$ or $\ln\alpha$ and $1/T$ for (*R*/*S*)-CHMA and (*R*/*S*)-MCHMA are excellent (Table IV), indicating that the differences of enthalpic changes (ΔH) for (*R*/*S*)-CHMA and (*R*/*S*)-MCHMA enantiomers were invariable over the entire temperature range studied. It was suggested that the chiral recognition mechanism for CHMA and MCHMA on HP-β-CD did not change over the entire temperature range studied. Table IV also shows that the enthalpic changes (ΔH) for CHMA and MCHMA in the HPLC system using HP-β-CD as chiral additives are negative, which indicates that the enantioseparation of CHMA or MCHMA in the studied chromatographic system is exothermic and the transfer of solutes from the mobile phase to the CSP is enanthalpically favored. Although the differences of the enthalpic changes [$\Delta(\Delta H)$] between the second-eluted enantiomer and the first-eluted enantiomer for CHMA and MCHMA are both negative, the differences of the entropic

Table VI
Partial Electron Donor Orbitals, Electron Acceptor Orbitals and the Corresponding $E^{(2)}$ Energies, Distances and Angles for (*R*/*S*)-CHMA–HP-β-CD Complexes Calculated by NBO Analysis at the B3LYP/6-31G Level*

(*R*)-CHMA–HP-β-CD					(*S*)-CHMA–HP-β-CD				
Electron donor	Electron acceptor	d (Å)	Angle (°)	$E^{(2)\dagger}$	Electron donor	Electron acceptor	d (Å)	Angle (°)	$E^{(2)}$
Within CHMA									
LP(2)O225	BD*(1)O235-H236	2.149	101.0	1.64	LP(2)O225	BD*(1)O235-H236	2.080	105.3	2.46
LP(2)O235	BD*(1)O225-H226	1.933	117.09	4.16	LP(2)O235	BD*(1)O225-H226	1.956	114.9	2.60
From CHMA to HP-β-CD									
LP(1)O225	BD*(1)C47-H157	2.236	152.5	0.92	LP(2)O225	BD*(1)C3-H129	2.342	163.4	1.11
LP(2)O225	BD*(1)C47-H157			2.91	LP(1)O234	BD*(1)C60-H166	2.618	166.1	0.85
LP(1)O234	BD*(1)C60-H166	2.224	176.3	0.63	LP(1)O234	BD*(1)C72-H175	2.274	126.2	1.60
LP(2)O234	BD*(1)C60-H166			1.08	LP(2)O234	BD*(1)C72-H175			0.87
LP(1)O234	BD*(1)C71-H173	2.612	123.7	0.55	LP(1)O235	BD*(1)C5-H131	1.927	151.7	6.22
LP(1)O235	BD*(1)C49-H159	1.920	167.9	3.45	LP(2)O235	BD*(1)C5-H131			2.24
LP(2)O235	BD*(1)C49-H159			0.94	LP(1)O235	BD*(1)C17-H140	2.195	144.1	1.06
BD(2)C219-C220	BD*(1)C58-H164			0.97	LP(2)O235	BD*(1)C17-H140			0.80
BD(1)C221-H238	BD*(1)C98-H184			0.54	BD(2)C220-C221	BD*(1)C69-H171			1.94
BD(2)C223-C224	BD*(1)C58-H164			1.17	BD(1)C220-H248	BD*(1)C58-H164			0.95
BD(1)C223-H240	BD*(1)C69-H171			0.56	BD(2)C222-C223	BD*(1)C107-H195			2.53
BD(1)C224-H241	BD*(1)C69-H171			0.65	BD(1)O225-H226	BD*(1)C3-H129			2.22
BD(1)O225-H226	BD*(1)C47-H157			0.56	BD(1)C230-H241	BD*(1)C36-H150			2.30
BD(1)C230-H247	BD*(1)C117-H20			0.55	BD(1)C230-H242	BD*(1)C25-H143			1.65
BD(1)C231-H244	BD*(1)C16-H138			5.98	BD(1)C231-H244	BD*(1)C25-H143			1.31
BD(1)C231-H245	BD*(1)C25-H143			0.94	BD(1)C231-H244	BD*(1)C27-H145			1.77
BD(2)C233-O234	BD*(1)C60-H166			1.45	BD(2)C233-O234	BD*(1)C71-H173			1.80
BD(1)O235-H236	BD*(1)C49-H159			3.98	BD(1)O235-H236	BD*(1)C17-H140			1.11
From HP-β-CD to CHMA									
LP(1)O7	BD*(1)C229-H248	2.711	138.8	0.53	LP(1)O20	BD*(1)O225-H226	2.282	139.4	3.32
LP(1)O31	BD*(1)C231-H245	2.063	134.7	2.96	LP(1)O20	BD*(1)O235-H236	2.238	128.7	2.79
LP(2)O31	BD*(1)C231-H245			0.58	LP(2)O20	BD*(1)O235-H236			1.03
LP(1)O53	BD*(1)O225-H226	2.666	123.3	0.60	LP(1)O42	BD*(1)C230-H241	2.478	119.9	0.56
LP(1)O64	BD*(1)O235-H236	2.108	119.8	5.09	LP(1)O42	BD*(1)C231-H244	2.468	120.5	0.70
LP(2)O64	BD*(1)O235-H236			1.33	LP(1)O62	BD*(1)C221-H249	2.470	149.0	1.52
LP(1)O74	BD*(1)C223-H240	2.394	137.0	0.57	LP(1)O110	BD*(1)C222-H250	2.472	118.9	0.59
LP(2)O110	BD*(1)C223-H240	2.593	149.8	1.26	LP(2)O110	BD*(1)C222-H250			0.66
BD(1)C16-H138	BD*(1)C231-H244			2.64	LP(2)O110	BD*(2)C222-C223			0.57
					BD(1)C3-H129	BD*(1)O225-H226			3.08
					BD(1)C17-H140	BD*(1)O235-H236			1.07
					BD(1)C25-H143	BD*(1)C231-C232			0.70
					BD(1)C25-H143	BD*(1)C231-H244			0.61
					BD(1)C27-H145	BD*(1)C231-H244			3.23
					BD(1)C36-H150	BD*(1)C230-H241			3.80

Note: BD denotes σ bonding orbital; BD denotes σ* antibonding orbital; LP denotes valence lone pair. For BD and BD*, (1) denotes σ orbital, (2) denotes π orbital. For LP, (1) and (2) denote first and second lone pair electrons, respectively. $E^{(2)}$ denotes the stabilization energy.
†Unit of $E^{(2)}$ is in kcal/mol.

changes [$\Delta(\Delta S)$] between the second-eluted enantiomer and the first-eluted enantiomer for CHMA and MCHMA are negative and positive, respectively. It is indicated that the (*S*)-CHMA–HP-β-CD system was more ordered than (*R*)-CHMA–HP-β-CD. Moreover, over the temperature range studied, the differences in the enthalpic and entropic changes for CHMA and MCHMA enantiomers in chromatographic separation process were fitted with $|\Delta(\Delta H)| > |T\Delta(\Delta S)|$, which indicated the enantioseparation of CHMA and MCHMA was an enthalpy-driven processes.

Molecular modeling and NBO analysis

To understand chiral recognition of enantiomers of CHMA and MCHMA on HP-β-CD, the inclusion interactions between HP-β-CD and each enantionmer of CHMA and MCHMA were further studied using molecular modeling techniques, and NBO analysis were carried out to complement the experimental results. The molecular modeling results obtained by molecular docking using AutoDock are presented for the dominating configuration of inclusion complexes with minimum binding free energy (ΔG) in Table V. Table V shows that the intermolecular interaction energy (ΔE_1) of the (*R*)-CHMA–HP-β-CD complex is greater than that of the (*S*)-CHMA–HP-β-CD complex as the ΔE_1 value of the (*S*)-MCHMA–HP-β-CD complex is greater than that of the (*R*)-MCHMA–HP-β-CD complex, indicating that the (*S*)-CHMA–HP-β-CD and (*R*)-MCHMA–HP-β-CD complexes are more stable than (*R*)-CHMA–HP-β-CD and (*S*)-MCHMA–HP-β-CD complex; this is consistent with the results observed in chromatographic experiments. Meanwhile, the $\Delta(\Delta G)$ value is in order of (*R*/*S*)-CHMA–HP-β-CD > (*R*/*S*)-MCHMA–HP-β-CD, impling that the enantioselection of (*R*/*S*)-CHMA on HP-β-CD is better than that of (*R*/*S*)-MCHMA, which is consistent with the results observed in chromatographic experiments, namely, that $\alpha_{(R/S)\text{-CHMA}}$ is greater than $\alpha_{(R/S)\text{-MCHMA}}$.

The dominating configurations for the (*R*/*S*)-CHMA–HP-β-CD and (*R*/*S*)-MCHMA–HP-β-CD complexes obtained by molecular docking using AutoDock are presented in Figure 3. As shown in Figure 3, although (*R*/*S*)-CHMA and (*R*/*S*)-MCHMA are both inserted into the HP-β-CD cavity from the wider rim of HP-β-CD, the binding geometries of these complexes are fully different. For the (*R*/*S*)-CHMA–HP-β-CD

Table VII

Partial Electron Donor Orbitals, Electron Acceptor Orbitals and the Corresponding $E^{(2)}$ Energies, Distances and Angles for (*R*/*S*)-MCHMA–HP-β-CD Complexes Calculated by NBO Analysis at the B3LYP/6-31G Level*

(*R*)-MCHMA–HP-β-CD					(*S*)-MCHMA–HP-β-CD				
Electron donor	Electron acceptor	d (Å)	Angle (°)	$E^{(2)\dagger}$	Electron donor	Electron acceptor	d (Å)	Angle (°)	$E^{(2)\dagger}$
Within MCHMA									
LP(1)O234	BD*(1)O225-H226	2.035	117.8	1.64	LP(2)O219	BD*(1)C225-H248	2.531	117.3	0.56
LP(2)O234	BD*(1)O225-H226	2.035	117.8	5.12	LP(2)O219	BD*(1)C228-H237	2.401	99.8	0.50
					LP(2)O234	BD*(1)O219-H220	2.082	116.9	3.57
					LP(1)O235	BD*(1)C221-H252	2.456	102.8	0.53
From MCHMA to HP-β-CD									
LP(1)O225	BD*(1)C5-H131	2.380	132.6	1.23	LP(1)O219	BD*(1)C49-H159	2.388	132.2	2.00
LP(2)O225	BD*(1)C3-H129	1.998	146.2	5.88	LP(2)O219	BD*(1)C38-H152	2.731	153.9	0.55
LP(1)O234	BD*(1)C14-H136	2.218	136.4	3.21	LP(1)O234	BD*(1)C36-H150	1.913	149.2	6.29
LP(1)O234	BD*(1)C16-H138	2.289	131.3	0.74	LP(2)O234	BD*(1)C36-H150			2.06
BD(2)C220-C221	BD*(1)O8-H78			1.33	LP(2)O235	BD*(1)C25-H143	2.399	140.6	0.83
BD(2)C220-C221	BD*(1)C107-H195			1.24	BD(1)C223-H244	BD*(1)C61-H167			0.69
BD(1)C220-H252	BD*(1)C3-H129			0.54	BD(1)C223-H245	BD*(1)C49-H159			0.59
BD(2)C222-C223	BD*(1)C69-H171			1.48	BD(1)C223-H245	BD*(1)C61-H167			3.15
BD(1)C223-H249	BD*(1)C58-H164			1.95	BD(1)C225-H248	BD*(1)C38-H152			1.56
BD(1)O225-H226	BD*(1)C3-H129			1.53	BD(1)C226-H251	BD*(1)C27-H145			3.01
BD(1)C229-H241	BD*(1)C49-H159			0.80	BD(2)C228-C229	BD*(1)C58-H164			2.33
BD(1)C229-H241	BD*(1)C61-H167			0.52	BD(1)C228-H237	BD*(1)C47-H157			0.68
BD(1)C229-H242	BD*(1)C61-H167			0.56	BD(1)C229-H238	BD*(1)C58-H164			2.35
BD(1)C231-H239	BD*(1)C38-H152			1.59	BD(2)C230-C231	BD*(1)C69-H171			1.85
BD(1)C231-H240	BD*(1)C38-H152			1.46	BD(1)C230-H239	BD*(1)C69-H171			2.33
BD(1)C232-H245	BD*(1)C16-H138			0.76	BD(1)C231-H240	BD*(1)C3-H129			1.47
BD(2)C233-O234	BD*(1)C16-H138			1.17	BD(2)C233-O234	BD*(1)C36-H150			1.22
BD(1)C236-H254	BD*(1)C25-H143			3.68					
From HP-β-CD to MCHMA									
LP(1)O20	BD*(1)O225-H226	1.830	151.9	16.66	LP(1)O9	BD*(1)C231-H240	2.448	129.9	1.05
LP(2)O20	BD*(1)O225-H226			1.05	LP(1)O22	BD*(1)C222-H243	2.531	126.7	0.74
LP(1)O22	BD*(1)C230-H238	2.724	144.8	0.66	LP(1)O22	BD*(1)C226-H250	2.127	138.5	1.94
LP(2)O22	BD*(1)C232-H245	2.718	145.9	0.64	LP(2)O22	BD*(1)C226-H250			1.67
LP(1)O62	BD*(1)C223-H249	2.747	137.4	0.50	LP(1)O31	BD*(1)C236-H253	2.299	128.9	2.08
BD(1)C3-H129	BD*(1)O225-H226			0.52	LP(1)O44	BD*(1)C225-H249	2.405	120.6	0.70
BD(1)C25-H143	BD*(1)C236-H254			2.61	LP(1)O53	BD*(1)O219-H220	2.219	111.9	2.92
BD(1)C58-H164	BD*(1)C223-H249			1.28	BD(1)C3-H129	BD*(1)C231-H240			2.63
BD(1)C109-H198	BD*(1)C221-H251			0.54	BD(1)O22-H81	BD*(1)C226-H250			0.84
					BD(1)C27-H145	BD*(1)C226-H251			1.08
					BD(1)C36-H150	BD*(2)C233-O234			0.50
					BD(1)C38-H152	BD*(1)C225-H248			0.68
					BD(1)C47-H157	BD*(1)C228-H237			0.70

Note: BD denotes σ bonding orbital; BD denotes σ* antibonding orbital; LP denotes valence lone pair. For BD and BD*, (1) denotes σ orbital, (2) denotes π orbital. For LP, (1) and (2) denote first and second lone pair electrons, respectively. $E^{(2)}$ denotes the stabilization energy.

†Unit of $E^{(2)}$ is in kcal/mol.

complexes, the phenyl and cyclohexyl groups in the CHMA molecule are located on the wider rim of HP-β-CD as the carboxylic acid moiety is located on the narrow rim of HP-β-CD. For the (*R*/*S*)-MCHMA–HP-β-CD complexes, the phenyl and ester groups in CHMA molecule are close to the wider rim of HP-β-CD as cyclohexyl group is located on the the narrow rim of HP-β-CD. It is indicated that the chiral recognition mechanism is closely related to the configurations of inclusion complexes.

To have a better estimation of the chiral recognition of HP-β-CD with (*R*/*S*)-CHMA and (*R*/*S*)-MCHMA, NBO analysis was carried out to predict hydrogen bonding between host and guest. In the NBO analysis, the stabilization energy [$E^{(2)}$] can be used to characterize the hydrogen bonding interaction between the LP(Y) lone pair of the proton acceptor and BD*(X–H) anti-bond of proton donor, which reflects the delocalization trend of electrons from electron donor to electron acceptor orbitals (39, 40). It is generally suggested that the $E^{(2)}$ value is larger than 2.0 kcal/mol for the strong hydrogen bonding interaction and from 0.5 to 2.0 kcal/mol for the weak hydrogen bonding interaction (41). The partial electron donor orbitals, electron acceptor orbitals and the corresponding $E^{(2)}$, distances and angles for (*R*/*S*)-CHMA–HP-β-CD and (*R*/*S*)-MCHMA–HP-β-CD complexes calculated by NBO analysis at the B3LYP/6-31G level are summarized in Tables 6 and 7. Tables 6 and 7 show that there are intermolecular hydrogen bonding interactions between (*R*/*S*)-CHMA and HP-β-CD in both inclusion complexes, suggesting that there are four strong hydrogen bonding interactions and six weak hydrogen bonding interactions in the (*R*)-CHMA–HP-β-CD complex, as there are three strong hydrogen bonding interactions and eight weak hydrogen bonding interactions in the (*S*)-CHMA–HP-β-CD complex. The H ··· O distances and angles at the H atom in these hydrogen bondings (O–H ··· O or C–H ··· O) herein range from 1.920 to 2.711 Å and from 118.9° to 176.3°, respectively, which fall within the reported data [less than 3.2 Å and greater than 90° (42)]. Similarly, there are three strong hydrogen bonding interactions and five weak hydrogen bonding interactions in the (*R*)-MCHMA–HP-β-CD complex as there are five strong hydrogen bonding interaction and five weak hydrogen bonding interactions in the (*S*)-MCHMA – HP-β-CD complex. It is also found that the $E^{(2)}$ values of intramolecular C–H ··· O

interactions for CHMA and MCHMA in complexes are greater than 2 kcal/mol, suggesting that there are intramolecular and intermolecular hydrogen bonding interactions in (*R*/*S*)-CHMA − HP-β-CD and (*R*/*S*)-MCHMA−HP-β-CD complexes. Additionally, there are many electron delocalization interactions of σ bonding orbital with antibonding orbital between host and guest molecules, indicating that the primary driving forces in the chiral recognitions of (*R*/*S*)-CHMA and (*R*/*S*)-MCHMA on HP-β-CD are hydrogen bonding interaction, dipole-dipole interaction, charge-transfer and hydrophobic interaction, which lead to the formation of different geometric structures of (*R*/*S*)-CHMA−HP-β-CD and (*R*/*S*)-MCHMA−HP-β-CD complexes.

Conclusion

Enantioseparations of (*R*/*S*)-CHMA and (*R*/*S*)-MCHMA can achieve baseline separation under selected chromatographic conditions, based on the formation of inclusion complexes of (*R*/*S*)-CHMA and (*R*/*S*)-MCHMA with HP-β-CD. The stoichiometry for (*R*/*S*)-CHMA−HP-β-CD and (*R*/*S*)-MCHMA−HP-β-CD complexes is 1:1. The chiral recognition of (*R*/*S*)-CHMA and (*R*/*S*)-MCHMA on HP-β-CD is dependent on the different configurations of inclusion complexes. However, the primary driving forces in the chiral recognitions of (*R*/*S*)-CHMA and (*R*/*S*)-MCHMA on HP-β-CD are hydrogen bonding interaction, dipole-dipole interaction, charge-transfer and hydrophobic interaction.

References

1. Xu, G.Y., Li, M.H., Liu, L.L.; *Pharmaceutical intermediate manual*. Chemical Industry Press, Beijing, China, (2000), pp. 164.
2. Vladimir, P., Zarko, S., Krunoslav, K.; Separation of enantiomers by partition between liquid phases; *Helvetica Chimica Acta*, (1982); 65: 377−384.
3. Tang, K.W., Miao, J.B., Zhou, T., Liu, Y.B., Song, L.T.; Reaction kinetics in reactive extraction for chiral separation of α-cyclohexyl-mandelic acid enantiomers with hydroxypropyl-β-cyclodextrin; *Chemical Engineering Science*, (2011); 66: 397−404.
4. Tang, K.W., Zhang, G.L., Huang, K.L., Li, Y.J., Yi, J.M.; Resolution of α-cyclohexyl-mandelic acid enantiomers by two-phase (O/W) recognition chiral extraction; *Science in China Series B-Chemistry*, (2007); 50: 764−769.
5. Guo, Z.F., Li, F.F., Xing, J.M.; Chiral recognition of α-cyclohexyl-mandelic acid in alcohol/salt-based a queous two-phase systems; *Chemical Journal of Chinese Universities*, (2011); 32: 275−280.
6. Huang, D.S., Huang, K.L., Chen, S.P., Liu, S.Q., Yu, J.G.; Enantioseparation of racemic α-cyclohexyl-mandelic acid across hollow fiber supported liquid membrane; *Journal of the Brazilian Chemical Society*, (2008); 19: 557−562.
7. Huang, D., Huang, K., Chen, S., Liu, S., Yu, J.; Racemic α-cyclohexyl-mandelic acid resolution across hollow fiber supported liquid membrane; *Chemical and Biochemical Engineering Quarterly*, (2008); 22: 447−452.
8. Feitsma, K.G., Drenth, B.F.H., de Zeeuw, R.A.; Comparison of two β-cyclodextrin bonded stationary phases for high-performance liquid chromatography; *Journal of Chromatography A*, (1987); 387: 447−452.
9. Shi, J.H., Ding, Z.J., Hu, Y.; Experimental and theoretical studies on the enantioseparation and chiral recognition of mandelate and cyclohexylmandelate on permethylated β-cyclodextrin chiral stationary phase; *Chromatographia*; (2011); 74: 319−325.
10. Jug, M., Kosalec, I., Maestrelli, F., Mura, P.; Analysis of triclosan inclusion complexes with β-cyclodextrin and its water-soluble polymeric derivative; *Journal of Pharmaceutical and Biomedical Analysis*, (2011); 54: 1030−1039.
11. He, Y.F., Shen, X.H., Chen, Q.D., Gao, H.C.; Characterization and mechanism study of micrometer-sized secondary assembly of β-cyclodextrin; *Physical Chemistry Chemical Physics*, (2011); 13: 447−452.
12. Shi, J.H., Yan, Y.; Separation of enantiomers of sec-butyl carboxylicates on β-cyclodextrin derivatives and chiral recognization mechanism; *Chinese Journal of Analytical Chemistry*, (2010); 38: 1450−1456.
13. Liu, P., Zhang, D.J., Zhan, J.H.; Investigation on the inclusions of PCB52 with cyclodextrins by performing DFT calculations and molecular dynamics simulations; *Journal of Physical Chemistry A*, (2010); 114: 13122−13128.
14. Shi, J.H., Jin, D., Xiao, K.K.; Separation of optical isomers of 2-chloropropionates on CycloSil-B chiral column; *Chinese Journal of Analytical Chemistry*, (2009); 37: 30−34.
15. Juvancz, Z., Kendrovics, R.B., Iványi, R., Szente, L.; The role of cyclodextrins in chiral capillary electrophoresis; *Electrophoresis*, (2008); 29: 1701−1712.
16. Shi, J.H., Cheng, X.W., Yan, W.; Enantiomeric separation of methylmandelate by gas chromatography and discussion the chiral recognition mechanism; *Chinese Journal of Pharmaceutical Analysis*, (2009); 29: 1681−1684.
17. Zhang, Q., Liu, Y.; Molecular recognition study of some aliphatic chiral enantiomers and dyes with β-cyclodextrin and its derivatives; *Chemical Journal of Chinese Universities*, (2004); 25: 458−461.
18. Berthod, A., Armstrong, D.W.; Multiple enantioselective retention mechanisms on derivatized cyclodextrin gas chromatographic chiral stationary phases; *Analytical Chemistry*, (1992); 64: 873−879.
19. Dodziuk, H., Lukin, O., Nowiński, K.S.; Molecular mechanics calculations of molecular and chiral recognition by cyclodextrins. Is it reliable? The selective complexation of decalins by β-cyclodextrin; *Journal of Molecular Structure-Theochem*, (2000); 503: 221−230.
20. Issaraseriruk, N., Shitangkoon, A., Aree, T.; Molecular docking study for the prediction of enantiodifferentiation of chiral styrene oxides by octakis(2,3-di-O-acetyl-6-O-tert-butyldimethylsilyl)-γ-cyclodextrin; *Journal of Molecular Graphics & Modelling*, (2010); 28: 506−512.
21. Zhou, Z.M., Li, X., Chen, X.P., Fang, M., Dong, X.; Separation performance and recognition mechanism of mono(6-deoxy-imino)-β-cyclodextrins chiral stationary phases in high-performance liquid chromatography; *Talanta*, (2010); 82: 775−784.
22. Shi, J.H., Xiao, K.K., Liu, Y.Y.; Host-guest interactions of β-cyclodextrin with enantiomers of ethyl α-chloropropionates; *Acta Physico-Chimica Sinica*, (2009); 25: 1273−1278.
23. Elbashir, A.A., Suliman, F.E.O., Saad, B.; Capillary electrophoretic separation and computational modeling of inclusion complexes of β-cyclodextrin and 18-crown-6 ether with primaquine and quinocide; *Biomedical Chromatography*, (2010); 24: 393−398.
24. Shi, J.H., Ding, Z.J., Hu, Y.; Theoretical study on chiral recognition mechanism of methyl mandelate enantiomers on permethylated β-cyclodextrin; *Journal of Molecular Modeling*, (2011); 18: 803−813.
25. Foresman, J.B., Frisch, A.; *Exploring chemistry with electronic structure methods (2nd edition)*. Gaussian, Inc., Pittsburgh, PA, (1996), pp. 39−59.
26. Morris, G.M., Goodsell, D.S., Halliday, R.S., Huey, R., Hart, W.E., Belew, R.K., Olson, A.J.; *Autodock, version 4.0.1*. The Scripps Research Institute, La Jolla, CA, (2007).
27. Gasteiger, J., Marsili, M.; Iterative partial equalization of orbital electronegativity—A rapid access to atomic charges; *Tetrahedron*, (1980); 36: 3219−3228.
28. Tiwari, R., Mahasenan, K., Pavlovicz, R., Li, C., Tjarks, W.; Carborane clusters in computational drug design: A comparative docking evaluation using AutoDock, FlexX, Glide, and Surflex; *Journal of Chemical Information and Modeling*, (2009); 49: 1581−1589.

29. Steffen, A., Thiele, C., Tietze, S., Strassnig, C., Kämper, A., Lengauer, T., *et al.*; Improved cyclodextrin-based receptors for camptothecin by inverse virtual screening; *Chemistry – A European Journal*, (2007); 13: 6801–6809.
30. Reed, A.E., Curtiss, I.A., Weinhold, F.; Intermolecular interactions from a natural bond orbital, donor-acceptor viewpoint; *Chemical Reviews*, (1988); 88: 899–926.
31. Chocholoušová, J., Špirko, V., Hobza, P.; First local minimum of the formic acid dimer exhibits simultaneously red-shifted O–H . . . O and improper blue-shifted C–H . . . O hydrogen bonds; *Physical Chemistry Chemical Physics*, (2004); 6: 37–41.
32. Ravelet, C., Geze, A., Villet, A., Grosset, C., Ravel, A., Wouessidjewe, D., *et al.*; Chromatographic determination of the association consrants between nimesulide and native and modified β-cyclodexttins; *Journal of Pharmaceutical and Biomedical Analysis*, (2002); 29: 425–430.
33. Chen, D.Y., Chen, Y.Y., Hu, Y.Z.; Study on chiral selective inclusion and retention characteristics of cis-trans isomers and enantiomers of sertraline with HP-β-CD as a mobile phase modifier; *Chinese Journal of Chromatography*, (2004); 22: 595–600.
34. de la Pena, A.M., Ndou, T.T., Anigbogus, V.C., Warner, I.M.; Solution studies of beta-cyclodextrin-pyrene complexes under reversed-phase liquid chromatographic conditions: Effect of alcohols as mobile-phase comodifiers; *Analytical Chemistry*, (1991), 63: 1018–1023.
35. Yao, Y., Liao, Q.F., Zeng, L.Y., Zhang, L., Ma, Y., Zeng, Y.E.; Determination of apparent oil-water partition coefficient of andrographolide and dehydroandrographolide and effect of pH on them; *Journal of Chinese Medicinal Materials*, (2009), 32: 1610–1612.
36. Lv, C.G., Zhou, Z.Q.; Chiral HPLC separation and absolute configuration assignment of a series of new triazole compounds; *Journal of Separation Science*, (2011); 34: 363–370.
37. Weng, W., Zeng, Q.L., Yao, B.X., Lin, W.S., Wang, Q.H., You, X.L.; Enantioseparation of amino acid derivatives with a cellulose-based chiral stationary phase; *Chromatographia*, (2006); 64: 463–467.
38. Cornell, W.D., Cieplak, P., Bayly, C.I., Gould, I.R., Merz, K.M., Ferguson, D.M., *et al.*; A second generation force field for the simulation of proteins, nucleic acids, and organic molecules; *Journal of the American Chemical Society*, (1995); 117: 5179–5197.
39. Mukherjee, V., Singh, N.P., Yadav, R.A.; Optimized geometry and vibrational spectra and NBO analysis of solid state 2,4,6-tri-fluorobenzoic acid hydrogen bonded dimer; *Journal of Molecular Structure*, (2011), 988: 24–34.
40. Madi, F., Khatmi, D., Dhaoui, N., Bouzitouna, A., Abdaoui, M., Boucekkine, A.; Molecular model of CENS piperidine β-CD inclusion complex: DFT study; *Comptes Rendus Chimie*, (2009); 12: 1305–1312.
41. Uccello-Barretta, G., Balzano, F., Sicoli, G., Fríglola, C., Aldana, I., Monge, A., *et al.*; Combining NMR and molecular modelling in a drug delivery context: investigation of the multi-mode inclusion of a new NPY-5 antagonist bromobenzenesulfonamide into β-cyclodextrin; *Bioorganic & Medicinal Chemistry*, (2004); 12: 447–458.
42. Leung, M.K.; Hydrogen bond—The dwarf in chemical bonding; *Chemistry (Chinese Chemical Society Taipei)*, (2004); 62: 43–58.